THERMAL SHOCK RESISTANCE OF A SODA LIME GLASS

Z. MALOU*, **,#M. HAMIDOUCHE*, **, N. BOUAOUADJA***, J. CHEVALIER****, G. FANTOZZI****

**Unité de Recherche Matériaux Emergents, Université Sétif 1, 19000 Algérie*
*** Institut d'Optique et Mécanique de Précision, Université Sétif 1, 19000 Algérie*
**** Laboratoire des Matériaux Non Métalliques, Institut d'Optique et Mécanique de Précision, Université Sétif 1, 19000 Algérie*
***** Université de Lyon, Laboratoire MATEIS, INSA Lyon, Villeurbanne, 69621 France*

#E-mail: mhamidouche@univ-setif.dz

Submitted October 6, 2012; accepted April 21, 2013

Keywords: Thermal shock, Thermal properties, Thermal stress, Numerical simulation

We studied the thermal shock of a three millimeters thickness soda lime glass using the hot-cold thermal shock technique. The cooling was made by ambient air jet on previously warmed samples. The heat transfer coefficient was about 600 W/°C.m^2 (Biot number $\beta = 0.3$). The thermal shock duration was fixed at 6 seconds. The hot temperature was taken between 100°C and 550°C while the cold temperature of the air flux was kept constant at 20°C. The acoustic emission technique was used for determining the failure time and the critical temperature difference (ΔTC). By referring to experimental results, thermal shock modelling computations are conducted. Our aim is especially focused on the fracture initiation moments during the cooling process and on the crack initiation sites. The used modeling is based on the local approach of the thermal shock during the experimental data treatment. For each test, the temperature profile and the transient stress state through the samples thickness are determined. By applying the linear superposition property of the stress intensity factors, evolution of the stress intensity factor KI in function of the pre-existing natural flaws in the glass surface is established. The size of the critical flaw is determined by the linear fracture mechanics laws. Computation results confirm the experimental values of the critical difference temperature obtained that is the source of the glass degradation.

INTRODUCTION

Because of the glass brittleness, the presence of superficial micro-cracks makes it very sensitive to mechanical and thermal solicitations [1]. The fracture is initiated at critical surface flaws [2].

During a thermal shock, a transient temperature gradient occurs, inducing thermal stresses. The shock intensity is related to the level of temperature difference between the initial temperature and that of the environment. There is a distinction between a cold-hot and a hot-cold thermal shock test. This later is more harmful for brittle materials because it generates tensile stresses on the rapidly cooled surface. These stresses may be sufficient to activate pre-existing micro-cracks and lead to materials damage or fracture.

The first theoretical description of thermal shock was proposed by Kingery [3]. He used a thermo-elastic analysis to define the critical temperature difference initiating fracture. This approach is focused on the conditions that control the fracture nucleation. Another approach was proposed by Hasselman [4] who treats the crack propagation rather than the crack nucleation. His theory enables to characterise the critical temperature difference as well as the damage state of the material. Hasselman takes into consideration the pre-existing cracks instability in relation with the temperature difference. On the other hand, Manson [5] introduced the Weibull distribution in the case of thermal shock. He showed that the stress level on the surface is higher than the expected values for high probability of fracture. A more realistic approach known as the local approach in comparison with the preceding global approaches [3-5] was proposed by EVANS [6] and completed by SHNEIDER [7]. This model gives numerically some new possibilities and a more precise description of the thermal shock. It is based on a thermo-elastic analysis by integrating the material defaults size to quantify the damage. This fine analysis enables to treat the processes occurring during the thermal shock. It takes into account the transitory character of the thermal shock by determining at every instant the transient temperature profile, the corresponding transient stress state and the stress intensity factor in relation with the crack size. The flowchart in figure 1 summarises the different approach steps.

Experimental methods used for controlling thermal shock damage are numerous [8-10]. There are static methods for measuring the material scaling, the weight loss and the mechanical strength deterioration. Other dynamic methods allow controlling the damage by measuring the frequency disturbances and the stationary or moving waves damping caused by the thermal shock.

In this work, thermal shock tests were undertaken on a soda lime glass in order to understand its behaviour toward sudden temperature variations.

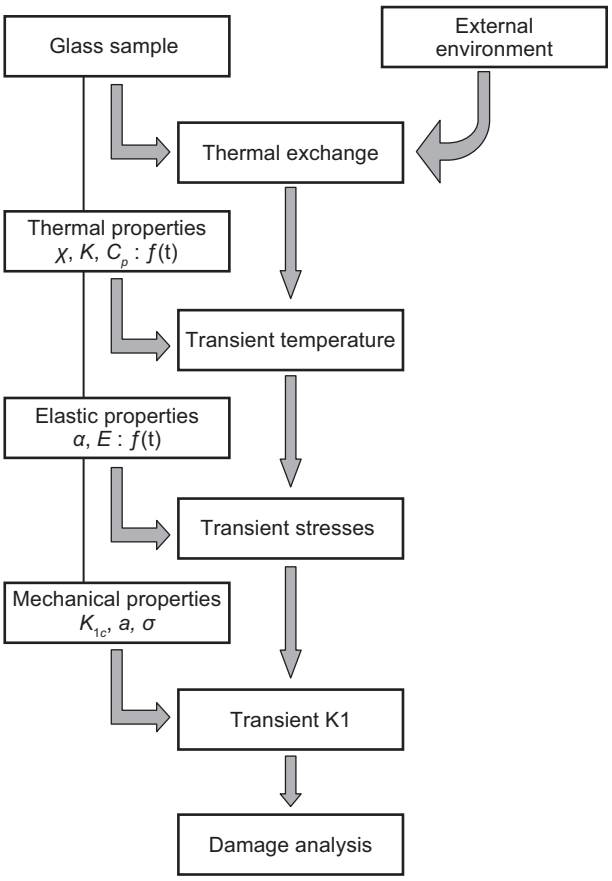

Figure 1. Diagram showing the three transitory stages of the thermal shock.

EXPERIMENTAL

A common silica-soda lime glass (thickness $e = 3$ mm) is used in this study. Its mean chemical composition comprises: 72.2 % SiO_2; 15 % Na_2O; 6.7 % CaO; 4 % MgO; 1.9 % Al_2O_3 and 0.2 % of impurities. The glass characteristics are gathered in Table 1. After the cutting operation, all the samples were rectified to the dimensions ($3\times15\times50$ mm^3). The large surface of the samples is used for soft thermal shock tests. The edges of the samples were chamfered by grinding. This operation is necessary to limit their effect during the mechanical and thermal shock tests. In order to eliminate residual stresses, the samples were annealed at 550°C during 30 min.

The device used for soft thermal shock tests is shown on Figure 2. The hot part is made up of a Pyrox furnace that can receive air blast. The samples are systematically cooled using a compressed air blast under a pressure of 4 bars applied on their two large surfaces. The sample holder allows the transfer between the cold and the hot zones using a pneumatic jack. The other function of the sample holder is the reception of the acoustic activity (piezoelectric sensor) during thermal shock tests. Good characteristics (resistance to thermal shock and fatigue, oxidation resistance and a low thermal conductivity) enable the wave guide to ensure a good coupling between the hot sample and the cold piezoelectric sensor. Ceramic foam is used as an acoustic and thermal insulator between the sample and the sample holder. Two thermocouples allow the measurement of the furnace temperature and that of the sample. A computer enables to record the acoustic activity and control the operations handling.

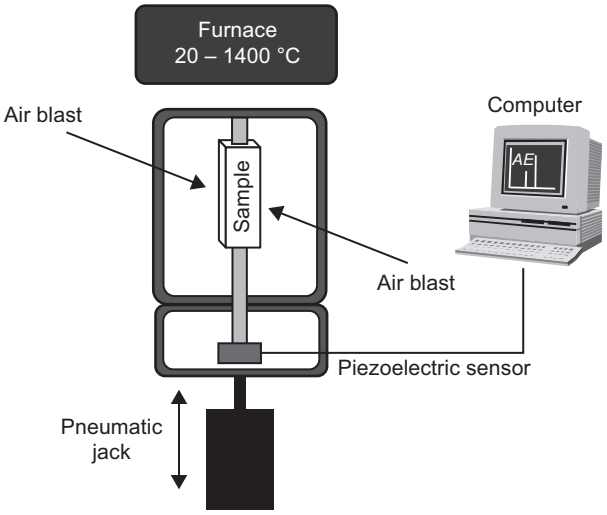

Figure 2. Schematic apparatus used for soft thermal shock tests (air blast).

Table 1. Main characteristics obtained at ambient temperature for the studied glass.

Properties	Values and units	Measurement technique
Elastic modulus E	72 GPa	Grindo-sonic
Linear expansion coefficient α	9.10^{-6} °C^{-1}	Dilatometer
Density	2.5 g/cm^3	Helium pycnometer
Vickers hardness HV	5.6 GPa	Durometer
Transition temperature T_g	550°C	Dilatometer
Poisson's Coefficient	0.22	Ultrasonic wave
Toughness K_{IC}	0.75 MPa.m$^{1/2}$	S.E.N.B.

The test made is a descendant thermal shock test type. Its severity is expressed in term of the Biot number (β = 0.3). We used a heat transfer coefficient h = 600 W/m^2.°C [10].

During the thermal shock tests, the samples were placed on a movable sample handler device. This device can be introduced or extracted from the kiln used. It allows the samples transfer between cold and hot enviroments by the use of a pneumatic jack. When the desired hot temperature is reached, a dwell time of 10 minutes at this temperature is necessary for homogenising the sample temperature. The cooling process is made by air jet at a temperature of 20°C during 6 seconds. The air pressure was kept constant at 4 bars. The sensor of the acoustic activity during a thermal shock is made of a piezo-electrical probe. The material wave guide does not dis-turb the acoustic emission signals during thermal shock tests.

The mechanical strength of the shocked samples was determined using a four point bending configuration. The inner and the outer span are respectively 10 and 35 mm. The tests were carried out in air using an Instron testing machine with a crosshead speed of 0.5 mm/min. Young's modulus was measured by the resonance frequency method using a Grindo-Sonic type apparatus.

For the modeling, we have taken into account the transitory aspect of thermal shock by integrating the evolution of thermo-elastic properties of glass during cooling.

To study thermal expansion, a test was carried out from ambient temperature up to 600°C in a silica sample holder dilatometer. The coefficient of thermal expansion over the range of temperature from 25 to 550°C was fitted to a polynomial:

$$\alpha\,(T) = 9.10^{-9} + 2.10^{-9}\,T \quad (°C^{-1}) \qquad (1)$$

where T is the absolute temperature.

Young's modulus E was measured as a function of temperature by the resonance frequency in bending:

$$E(T) = 72 - 6.61\,T - 0.016\,T^2 - 10^{-5}\,T^3 \quad \text{(GPa)} \qquad (2)$$

Thermal conductivity was obtained from literature [11]. In the range from 20 to 800°C it can be fitted by:

$$K = 1.576 + 9\times10^{-4}\,T - 3\times10^{-6}\,T^2 \quad \text{(W/m/°C)} \qquad (3)$$

The specific heat Cp was also derived from literature [12] since it is mostly dependent on the chemical composition:

$$Cp = 217.7 + 1.01\,T - 8.10^{-4}\,T^2 \quad \text{(J/kg/°C)} \qquad (4)$$

Poisson's coefficient, being weakly dependent on the temperature, was only measured at room temperature by the wave velocity method which yielded to the value (v = 0.22).

During the tests, when a sample reaches the desired hot temperature, the cooling process is made by air jet at a temperature of 20°C during 6 seconds.

A software package based on a Turbo Pascal program is used. It enables to evaluate the transient temperatures and the transient stresses at every instant of the thermal shock and at any position on the sample.

By referring to experimental results (acoustic emission, Young's modulus and mechanical strength after damage), the computations were focused on particular cases. The fracture initiation moments during the cooling process and the crack initiation site are especially studied.

The modelling is based on the local approach of the thermal shock. The model used is presented in Figure 3. The transitory temperature distribution is first determined. The transitory superficial stresses and the stress intensity factor (F_{IC}) using the principle of superposition [13] are then evaluated. The temperature dependence of the thermo-elastic properties were integrated In this numerical procedure. It enables to evaluate the transient temperatures and the transient stresses at every instant of the thermal shock and every point on the sample thickness.

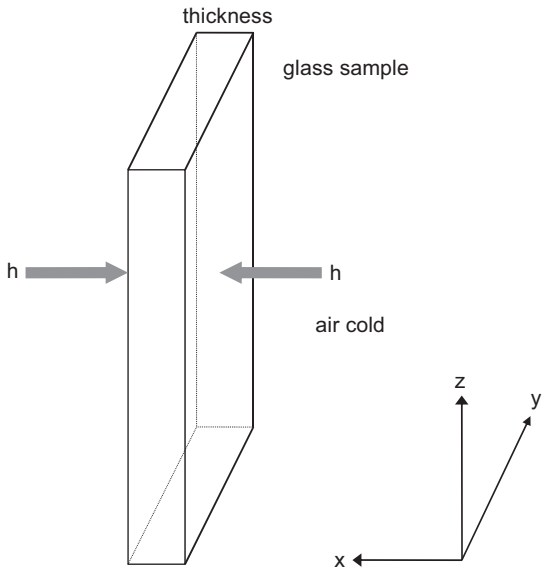

Figure 3. Schematised used model.

RESULTS AND DISCUSSION

Experimental results

Figure 4 shows that the relative mechanical strength remains constant up to a temperature difference of 270°C. Beyond this limit, it decreases sharply. This rapid strength variation indicates the critical temperature difference causing the glass damage. This temperature difference corresponds to the cracks propagation located at the frontal face (15 × 50 mm^2) of the tested specimen.

From these results, we notice that strength tests can also be used to characterise the critical temperature difference (ΔT_C = 270°C). A small scattering of strength values was observed for temperature variations greater

than ΔT_C (the critical temperature difference). This is statistically related to the distribution of the cracks induced by thermal shock (size and position distribution) [14].

For temperature difference greater than 270°C, the decrease of the relative stress is less pronounced. The relative strength (after the thermal shock test) is about 20 % for a cold air quench at a temperature difference of 380°C. This shows that soda lime glass has a fairly bad thermal shock damage resistance.

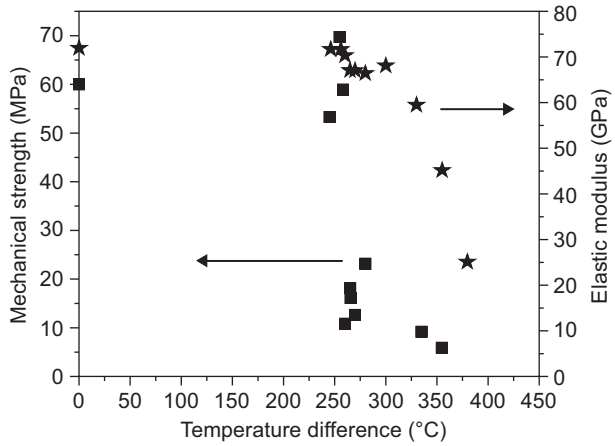

Figure 4. Variation of mechanical strength and dynamic elastic modulus of glass samples submitted to thermal shock versus temperature difference ΔT.

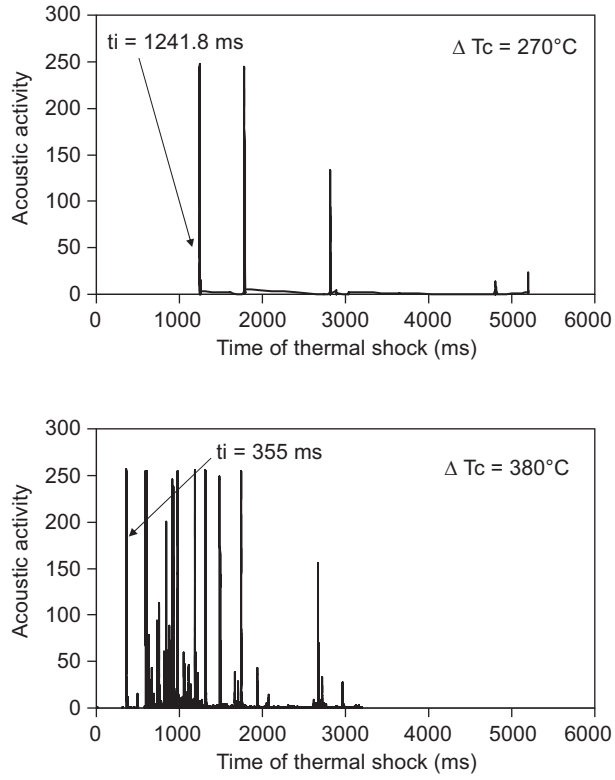

Figure 5. Normalised acoustic emission activity recorded for glass samples thermally shocked during 6 s by air at two temperature differences (ΔT_c = 270°C, ΔT = 380°C).

On the other hand, the same Figure 4 shows that the Young's modulus variation is rather smooth (without any sudden change) comparing to the strength variation. There is a regular and less pronounced decrease. Critical temperature difference cannot be predicted from Young's modulus results. This property is more sensitive to defects present in the sample volume.

Figure 5 shows an example of acoustic emission registered during the thermal shock (6 seconds) for a critical temperature difference (ΔTc = 270°C) and for an over-critical temperature differences (ΔT = 380°C). It clearly appears that when the shock severity increases, the emitted acoustic event number becomes more important. This relation is governed by the released energy for creating new surfaces during the propagation of the most critical flaw. This result shows that the acoustic emission control is in good accordance with the strength results.

The number, the amplitude and the acoustic emission initiation time are very sensitive to the fixed temperature difference (Figure 6). The events number can then be related to the crack dimensions (length and depth) induced by the thermal shock.

When the temperature difference is large, the generated stresses become more important leading therefore to a precocious early cracking occurring at the beginning of the cooling process. A relation exists between the initial thermal shock temperature and the acoustic events number. We can notice that the emission initial time of the first event is directly dependent on the difference temperature of the thermal shock.

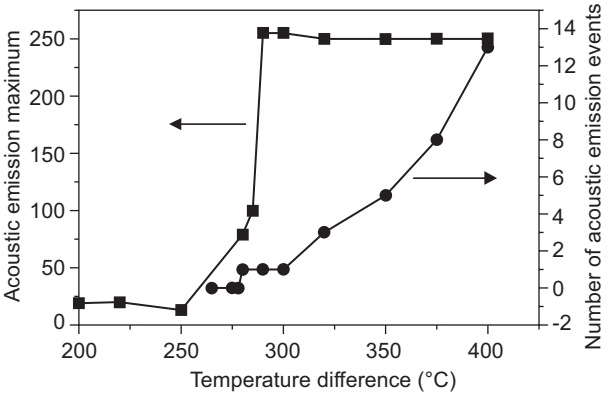

Figure 6. Acoustic emission echoes number and normalised acoustic emission maximum versus temperature difference (3 mm thickness sample).

Modelling results

During experimental tests, the damage starts at the critical temperature difference of 270°C and it lasts at a cooling time of 1241.8 ms. The acoustic emission characterising the material damage occurred at this particular instant (t = 1241.8 ms) of the critical thermal shock. Therefore, our modelling is limited to these

critical thermal shock conditions leading to the material damage. Transient temperatures and transient stresses computations were conducted at the instant and the site where the crack appears.

First of all, the temperature difference (T_c – T_s) between the sample inner center (x = 1.5 mm) and its surface (x = 0) in function of the cooling duration is determined for ΔT_c = 270°C. Figure 7 shows that this temperature difference (center-surface) starts by an increase from the thermal shock beginning up to a maximum before diminishing and reaching the thermal equilibrium.

At the critical instant (t = 1241.8 ms), the superficial temperature of the sample is 221°C, whereas that of the sample centre is 277.7°C. The transient temperature difference between the surface and the sample centre for every instant during the cooling process is determined for a starting thermal shock temperature of 290°C. The maximal temperature difference (T_c – T_s) is about 56.8°C after a cooling time of 1440 ms. This time is of the same order than that obtained by acoustical emission corresponding to the moment when the first crack appears.

Using transient temperatures, we numerically computed the transitory stresses using linear elasticity equations. In these computations, we also considered the temperature dependence of the elastic properties as the crack appears. The maximum tensile stress is obtained on the largest face of the specimen, precisely in the middle of this face where the cracks propagation was observed.

Figure 8 represents the transient stresses evolution σ (0, t) at the surface for the critical thermal shock. This superficial stress reaches its maximum at 34 MPa after a cooling time of 1440 s. The superficial stress value calculated corresponds to the stress decrease in the mechanical strength at the critical temperature difference observed in the experimental results.

Figure 9 shows the transient stresses evolution in function of the depth for different cooling durations on a soda lime glass cooled from a temperature of 290°C to 20°C during 6 s. We can see that tensile stresses are maximal on the surface and diminish with depth. They become compressive after a depth corresponding to x = = *(1/5)e*, with "*e*" is thickness. The compressive stress at the glass center is about half the maximum tensile stress at the surface. The stress envelop curve is obtained for the maximal temperature difference (T_c – T_s), obtained after 1440 ms cooling time.

The stress intensity factor was evaluated with the hypothesis of a unidirectional crack propagation submitted to the stress profile $\sigma_{xx}(x, t)$ according to Wu's calculation [13].

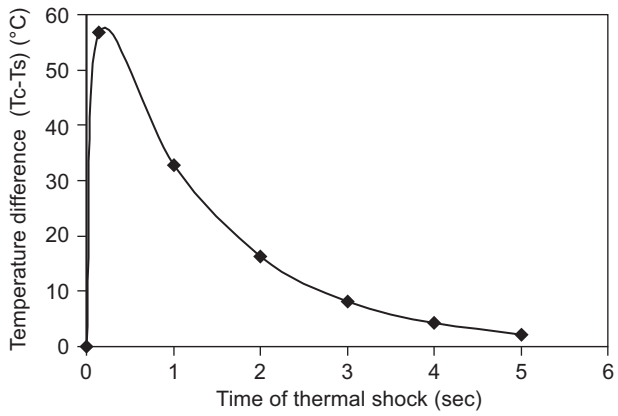

Figure 7. Temperature difference (T_c – T_s) in function of the cooling duration for the critical thermal shock (soda lime glass thickness is 3 mm).

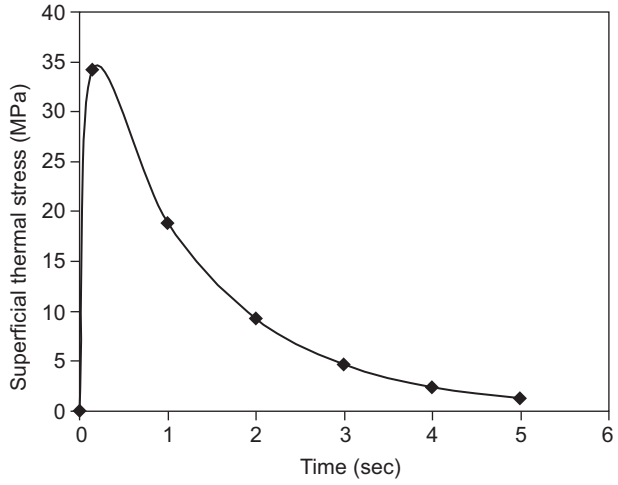

Figure 8. Transient surface stress σ (calculated with the transient temperature in figure 7) versus cooling duration of soda lime glass shocked by air jet at ΔT_c = 270°C.

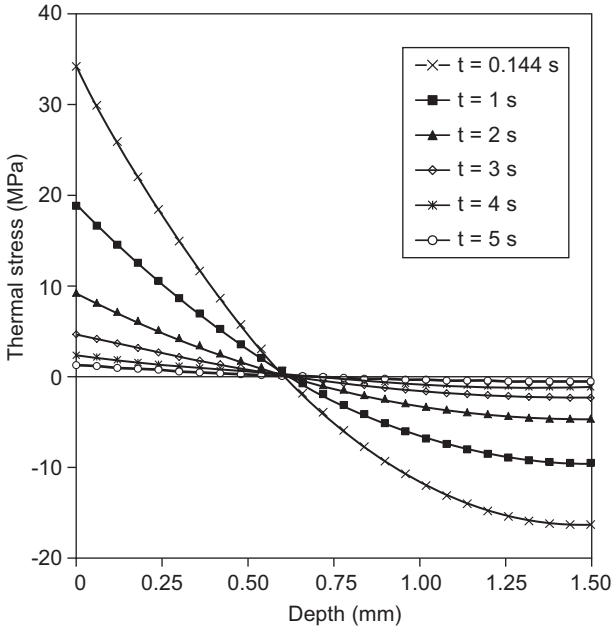

Figure 9. Transient stress σ in function of depth down to the center at different thermal shock times, for a temperature difference (ΔT_c = 270°C), and a sample thickness e = 3 mm.

In Figure 10, we represented the stress intensity factor *K(a, t)* variations with crack depth for the transient stress distributions showed in Figure 9. The envelope of the curves has a maximum at the time t = 1440 ms. The stress intensity factor *K(a, t)* is greater than the critical value K_{IC} for that time and a flaw size of 49 µm. This critical flaw size was determined according to the relation:

$$K_{IC} = \sigma_r \cdot y \cdot \sqrt{a_c} \qquad (5)$$

where y is the shape factor, σ_r is the fracture strength of the material, a_c is the critical flaw size, K_{IC} is the fracture toughness.

The critical flaw size a_c was determined using the ambient temperature corresponding to the surface temperature at the time 1440 ms. At the end of the thermal shock, a flaw of 49 µm size will reach a final length a_f corresponding to 1350 µm. The experimental results showed that the critical thermal shock would reduce the initial stress to about 30 %. The difference is probably related to the cracking mode. As the critical thermal shock induces only one crack through the sample, we used in this study the opening mode for the determination of the critical flaw size.

Knowing that there are no toughening mechanisms in the sample glass, the stress intensity factor remains the only criterion for characterising the thermal damage.

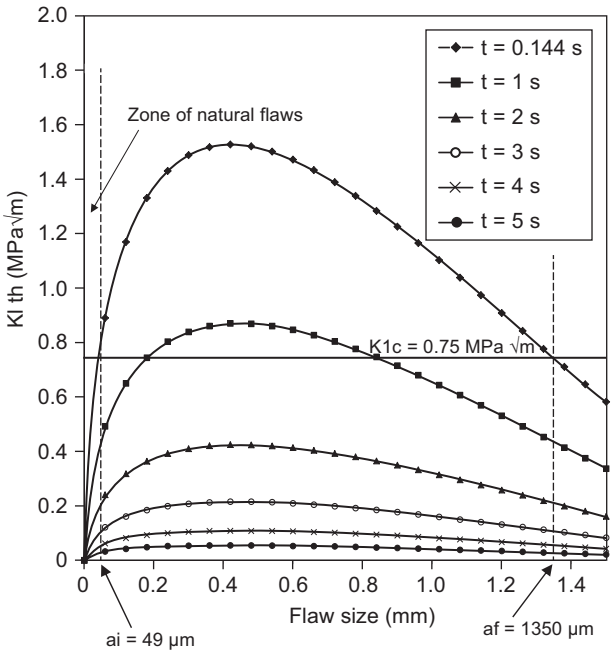

Figure 10. Critical thermal shock (ΔT = 270°C) generated thermal stress intensity factor K_{IC} of soda lime glass (thickness = 3 mm) versus crack length for a Biot number of 0.3 and a range of cooling time.

CONCLUSION

Glass with a 3 mm thickness presents a critical difference temperature ΔT_C = 270°C in the case of descending thermal shock characterized by a Biot number β = 0.3 and a heat transfer coefficient h = 600 W/m^2.°C.

Thermal shock damage control made by acoustic emission leads to results similar to those obtained by measuring the residual strength. The acoustic events number and the emission starting duration are directly related to the thermal shock severity.

The critical temperature difference cannot be predicted from Young's modulus results, this property being is more sensitive to bulk sample defects.

For the imposed critical temperature gradient ΔT_c = 270°C and at the critical instant (t = 1241.8 ms), the temperature difference between the surface and the sample ($T_c - T_s$) is about 56.8°C. The compressive stress at the glass center is about half the maximum tensile stress at the surface. The surface thermal stresses leading to the fracture are less than the mechanical strength of the material. The thermal shock simulation by the local approach corresponds to the experimental results.

REFERENCES

1. Malou Z., Hamidouche M., Madjoubi M.A., Loucif K., Osmani H., Bouaouadja N.: Glass Technology *41,* 55 (2000).
2. Madjoubi M.A., Bousbaa C., Hamidouche M., Bouaouadja N.: Journal of the European Ceramic Society *19*, 2957 (1999).
3. Kingery W. D.: Jour. Amer. Ceram. Soc**.** *38*, 3 (1955).
4. Hasselman D. P. H.: J. Am. Ceram. Soc. *52*, 600 (1969).
5. Manson S. S., Smith R. W.: J. Amer. Ceram. Soc. *38*, 18 (1955).
6. Evans A. G.: Proc. Br. Ceram. Soc. *25***,** 217 (1975).
7. Schneider G. A.: Ceram. Inter *17***,** 325 (1991).
8. Simonneau A. M. : *Résistance aux chocs thermiques et à la fatigue thermique de céramiques thermomécaniques, influence des conditions expérimentales*, Doctorat thesis, University of Limoges 1989.
9. Mignard F., Olagnon C., Fantozzi G.: J. Eur. Ceram. Soc. *15***,** 651 (1995).
10. M. Hamidouche, N. Bouaouadja, C. Olagnon, G. Fantozzi: Ceramics International 29, 599 (2003).
11. Mc Lellan G.W., Shand E.B.: *Glass engineering hand book*, 1984.
12. Kingery W.D., Bowen H.K., Uhlman D.R.: *Introduction to ceramics*, Science and technology of Materials, 1976.
13. Wu X. R. in: *Thermal shock and thermal fatigue behaviour of advanced ceramics*, Ed. Shneider G. A., Academic Publisher, Germany 1992.
14. Malou Z., Hamidouche M., Bouaouadja N., Fantozzi G.: Ceramics-Silikáty 55, 215 (2011).